INDOOR MAPPING BASED ON TIME DELAY ESTIMATION IN WIRELESS NETWORKS

Hassan Naseri *Visa Koivunen*

Aalto University, School of Electrical Engineering, Finland ({firstname.lastname}@aalto.fi)

ABSTRACT

In indoor wireless localization, navigation and communications, knowledge of the floor plan is valuable side information and provides more reliable performance. Such information may not be available. Estimating indoor maps using sensor networks and time delay measurements, i.e., without angular information, is a challenging task. In this paper, a novel algorithm is developed to solve the problem of mapping and measurement clustering. The algorithm is applicable to wireless and acoustic networks with high resolution time delay measurements.

Index Terms— Mapping, Localization, Sensor Networks

1. INTRODUCTION

Geometrical models and maps of the indoor environment are vital to many applications such as indoor localization, emergency services and robot navigation. The performance of indoor wireless localization could be improved by exploiting the multipath propagation of radio signals. Such techniques require a map of the environment and clustering of the measurements [1–4]. In this paper, *map* denotes the geometry of the reflecting objects in a propagation environment. Multipath radio propagation may be modeled as a superposition of a line-of-sight (LOS) component, several deterministic specular components, and a random noise component [5, chap. 7]. Specular multipath components (MPCS) contain rich geometric information which can be used to estimate a map of the environment.

In this paper, the problem of estimating the geometry of the environment given high resolution time delay estimates between a number of nodes is addressed. Time delay estimates corresponding to single-bounce reflection (SBR) paths, i.e., first-order reflections, between the nodes and reflecting objects are employed. If angular information, e.g., directions-of-arrival of radio transmissions, are available the problem becomes much simpler. However, in this paper, only distance measurements obtained by time delay estimation are considered as inputs. In wireless networks, the lengths of specular paths can be estimated using high resolution time delay estimation techniques [6]. In order to get absolute distance estimates, a precise network synchronization algorithm is also needed to compensate for clock offsets and skews [7].

There is an ongoing research on ultra wide band (UWB) indoor mapping. A radar solution with simple antenna array was proposed in [8]. However, most wireless radios do not support radar operation; and monostatic radar solutions are not applicable to a network setup. Some algorithms were developed *exclusively for rectangular* rooms [9, 10]. They required testing all possible combinations of the measurements and walls to solve data association problem. Such a combinatorial complexity limits the scalability to a few nodes. The method proposed in [11] required delay estimation of second order reflections, which are in general very weak. It also had combinatorial complexity. An attempt to generate a 3D map by first estimating the angular information from time delays was presented in [12], which did not succeed to create a complete map. An approach based on synthetic aperture radar (SAR) process was proposed in [13]. They estimated scattering coefficient for every point in the coverage area of network. The method was based on averaging in delay domain, and did not employ a geometric model for reflections. Hence, it required a large number of measurements, and did not estimate a geometric map for the environment. The problem of indoor mapping using time delay measurements has been studied recently in the field of acoustics [14, 15]. However, they did not develop a complete algorithm for the case of multiple reflectors.

The contribution of this paper is to develop a low-complexity clustering algorithm to detect multiple reflectors and estimate their geometry using time delay measurements. The proposed algorithm employs image processing techniques to detect reflectors and estimate their geometry, followed by an iterative refinement stage. The algorithm has polynomial complexity, and only requires one snapshot of delay measurements between few nodes to estimate a map. To the best of authors' knowledge, there is no method in the literature with polynomial complexity to estimate the geometry of multiple reflectors using time delay measurements.

The rest of this paper is organized as follows. Section 2 states the problem and gives a geometric measurements model. The clustering algorithm based on Hough transform is described in section 3, and the refinement stage of the algorithm in section 4. A short discussion on the algorithm is included in section 5. Simulation results are presented in section 6. Finally, section 7 concludes the paper.

2. PROBLEM STATEMENT AND MODELING

Consider a wireless network of n users/nodes with known positions situated in a room with unknown floor plan, see figure 1. The nodes are transmitting and receiving signals cooperatively to estimate all pairwise radio channels, i.e., time delays of propagation paths, with high resolution. The problem is to estimate a map of the room using time delay estimates. It is assumed that the lengths of all, or most, SBR paths are given. A SBR path is a ray between two nodes with a single bounce at a reflector. Second or higher order reflections are not considered in the model because of their complex geometry and larger estimation errors [1]. Moreover, scattering and complex propagation mechanisms are not considered in the employed geometric model. The contributions of such processes may be incorporated into a random noise component and distance estimation error. The estimated path lengths are modeled as

$$\hat{r}_{(u,v,i)} = r_{(u,v,i)} + e, \quad (u, v, i) \in \mathcal{S}_{SBR}, \tag{1}$$

where $r_{(u,v,i)}$ is the Euclidean distance of the ray between nodes u, v reflected at reflector i, and $\mathcal{S}_{SBR}$ is the set of all such 3-tuples. Distance estimation error is modeled with a an additive zero-mean random term e. With n nodes and m reflectors, there are $mn(n-1)/2$ distinct SBR paths at most, i.e., $|\mathcal{S}_{SBR}| = O(mn^2)$. The reflectors are

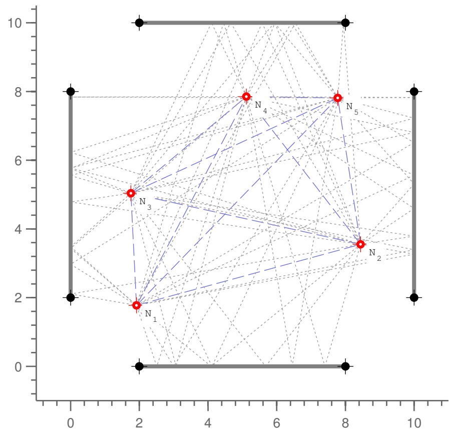

Fig. 1: A wireless network with five nodes situated in a room with four walls. The reflectors/walls are modeled with line segments. Single-bounce propagation paths between nodes are shown with dotted lines.

modeled in two dimensional space with a series of line segments, similar to a floor plan when the walls are piecewise straight. The objective is to find the geometry of such line segments given the set of SBR distance estimates. The locus of *reflection points* for a SBR path is an ellipse with foci at node positions and major axis equal to the path length. The reflector line is a tangent to such ellipse at reflection point [14], see figure 2. Hence, the geometry of reflector lines may be estimated by finding *common tangents* to the ellipses corresponding to each reflector. All ellipses corresponding to the SBR paths of figure 1 are illustrated in figure 3.

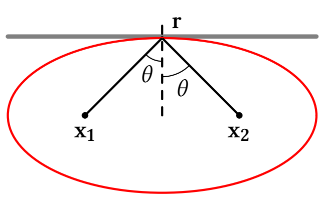

Fig. 2: The locus of a reflection point $\mathbf{r}$ for an SBR path with a given length is an ellipse with foci at node positions. The reflector line is a tangent to this ellipse.

In the Cartesian coordinate system, an ellipse is defined as the set of points (x, y) which satisfy the general equation of a conic section for non-degenerate cases, given by

$$ax^2 + bxy + cy^2 + dx + ey + f = 0, \tag{2}$$

provided that $b^2 - 4ac < 0$. The general equation's coefficients can be found given the foci, i.e., node positions, and the major axis r of the ellipse, i.e., SBR path length. Using homogeneous coordinates, the equation of an ellipse can be simplified, and the equation of a tangent line to ellipse may be formulated conveniently. In homogeneous coordinates, an ellipse is given by

$$\mathscr{C} = \{\mathbf{x} \in \mathbb{R}^3 \mid \mathbf{x}^{\mathrm{T}}\mathbf{C}\mathbf{x} = 0\}, \tag{3}$$

where $\mathbf{x} = [\lambda x, \lambda y, \lambda]$, and $\mathbf{C} \in \mathbb{R}^{3\times 3}$ is a *conic matrix* given by

$$\mathbf{C} = \begin{bmatrix} a & b/2 & d/2 \\ b/2 & c & e/2 \\ d/2 & e/2 & f \end{bmatrix}. \tag{4}$$

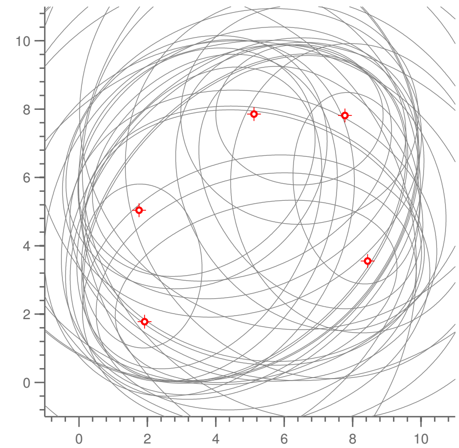

Fig. 3: The locus of reflection points for SBR delay estimates are ellipses; delay estimation error variance is 0.01. The geometry of reflector lines can be found by finding *common tangents* to the corresponding ellipses.

A line $\mathbf{l} = [\ell_1, \ell_2, \ell_3]$ in homogeneous coordinates is tangential to an ellipse if and only if

$$\mathbf{l}^{\mathrm{T}}\mathbf{C}^*\mathbf{l} = 0, \tag{5}$$

where $\mathbf{C}^* = |\mathbf{C}|\mathbf{C}^{-1}$ is the adjoint matrix of the conic matrix $\mathbf{C}$. The conic section defined by $\mathbf{C}^*$ is called the *line conic* associated with the *point conic* defined by $\mathbf{C}$. A common tangent to a set of q ellipses may be found by solving a system of quadratic equations given by $\mathbf{l}^{\mathrm{T}}\mathbf{C}_j^*\mathbf{l} = 0, \;\; j = 1, \ldots, q$. Since the distance estimates are not error-free, such a system of equations may not have an exact solution. The estimate of a common tangent $\mathbf{l}_i$ may be obtained in least-squares sense by minimizing the following cost function.

$$J_i(\mathbf{l}) = \sum_{j \in \mathcal{S}_i} \left\| \mathbf{l}^{\mathrm{T}}\mathbf{C}_j^*\mathbf{l} \right\|_2^2, \tag{6}$$

where $\mathcal{S}_i$ is the set of indices j of ellipses/paths corresponding to the reflector line $\mathbf{l}_i$. The partitioning of ellipses or distance estimates to such sets $\mathcal{S}_i$ are not given in advance, and need to be found by a clustering method.

3. INITIAL CLUSTERING

A variant of Hough transform [16] is used for initial clustering, i.e., finding common tangents to ellipses. A technique developed in this paper directly maps ellipse tangents to Hough space. The procedure is summarized in table 1, and the different stages are described in this section.

Table 1 Initial clustering procedure

1: **Sample tangent lines** to every ellipse.
2: **Quantize the lines** and add to a Hough accumulator.
3: **Detect intensity peaks** by smoothing and thresholding.
4: **Estimate cluster heads** by averaging.

3.1. Sampling

Hough transform maps a line in Cartesian coordinates to a point (ρ, θ) in Hough space, where ρ is the distance from the line to the origin, and θ is the angle of the line with respect to y-axis. In this paper, Hough transform is not computed for every single point in Cartesian space. Each ellipse is uniformly sampled by finding hundreds of points on it. Then the tangent to an ellipse at each of these points is transformed directly to Hough space. For every point (x, y) on an ellipse, the Hough transformation of the tangent line at that point is given by

$$\begin{aligned} \theta &= \Re\left(\tan^{-1} m\right) + \operatorname{sign}(y - mx)\pi/2, \\ \rho &= \left|x \cos\theta + y \sin\theta\right|, \end{aligned} \tag{7}$$

where m is the slope of tangent line at point (x, y). The parametric equation of an ellipse in Cartesian coordinates is given by

$$\begin{aligned} x(t) &= x_c + \alpha \cos t \cos\varphi - \beta \sin t \sin\varphi, \\ y(t) &= y_c + \alpha \cos t \sin\varphi + b \sin t \cos\varphi. \end{aligned} \tag{8}$$

The slope of a tangent line to the ellipse at point t is given by

$$m(t) = \frac{\beta \cos t \cos\varphi - \alpha \sin t \sin\varphi}{-\beta \cos t \sin\varphi - \alpha \sin t \cos\varphi}. \tag{9}$$

The sampling is done uniformly in angular domain $t \in [o, 2\pi)$.

3.2. Accumulation

All the transformed lines are then added to a Hough accumulator. The accumulator is a grid of discrete points in finite $[\rho, \theta]$ space. In the accumulation process, for each line the value of closest bin in the accumulator space is increased by one. This process is equivalent of finding a two-dimensional histogram with bins at the grid points. The value of each point/bin in the accumulator space, determines the number of lines mapped to that bin. The accumulator space, which will be referred to as *Hough image*, can be further processed as a grayscale image. The intensity peaks in the Hough image correspond to the common tangents to ellipses. The Hough space is periodic in θ direction, hence image processing techniques are applied after circular padding.

3.3. Detection

A two-dimensional Gaussian low-pass filter is applied to the acquired Hough image to smooth out quantization noise and the error in parameter space, i.e., distance estimates. Moreover, smoothing enhances large-scale structures. After filtration, the grayscale image is converted to a binary image by thresholding. The thresholding operation detects the intensity peaks in the Hough image. Then, the binary image is processed by morphological dilation to expand the areas of detected peaks. It also connects close-by regions and smooths the boundaries. Detecting large regions around peaks, instead of single points, is useful for later processing to mitigate errors by averaging. The output of detection stage is a binary mask of the clusters in Hough space.

3.4. Averaging

Each region in the binary mask corresponds to a common tangent. Cluster heads, i.e., common tangents, are found by applying the binary mask to the original grayscale Hough image. Then, a weighted center of mass for each region is found. Mass of each point is the pixel value in the grayscale Hough image. The Euclidean distance is used to find the center of mass. The extracted centroids are the initial estimates of the common tangents. If there are k region in the binary mask, the lines $\mathbf{l}_i$, $i = 1, \ldots, k$ are estimated as common tangents.

4. ITERATIVE REFINEMENT

The estimates found by Hough transform method are usually good, such that further processing may not improve them. However, an iterative refinement technique is proposed in this section to improve the initial estimates when measurement error is small. The technique consists of two steps, *assignment* and *fitting*. These two steps can be run for a single or few iterations until convergence. Convergence is achieved when there is no change in cluster memberships. The maximum number of iterations can be fixed to a small number.

4.1. Assignment

Assigning measurements to cluster heads, also known as echo labeling, is done by assigning each ellipse to the closest cluster head, i.e., common tangent. The distances between each ellipse and all cluster heads are found using the distance function given in (6). The cluster label for ellipse $\mathscr{C}_j$ is found by

$$L_j = \underset{i \in \{1, \ldots, k\}}{\arg\min} \left\| \mathbf{l}_i^{\mathrm{T}} \mathbf{C}_j^* \mathbf{l}_i \right\|_2, \tag{10}$$

where $\mathbf{l}_i$, $i = 1, \ldots, k$ are the estimated cluster heads in homogeneous coordinates. The label sets for clusters are constructed as $\mathcal{S}_i = \{j \mid L_j = i\}$.

4.2. Fitting

In this refinement stage, a new common tangent is found for each cluster analytically. The algorithm is given in [14], which is summarized as follows. The common tangent for cluster i is given by the following optimization problem.

$$\mathbf{l}_i = \underset{\mathbf{l}}{\arg\min}\, J_i(\mathbf{l}), \tag{11}$$

where $J_i(\mathbf{l})$ is a *non-convex* cost function given in (6). The global optimum can be found by slicing the problem into orthogonal planes. Any line in homogeneous coordinates intersects with one of the planes $\ell_1 = 1$ and $\ell_2 = 1$. Slicing $J_i(\mathbf{l})$ with the planes $\ell_1 = 1$ and $\ell_2 = 1$, and then setting the partial derivatives to zero gives two sets of local minima $\mathscr{L}_1$ and $\mathscr{L}_2$ as follows.

$$\mathscr{L}_1 = \left\{ \mathbf{l} : \frac{\partial J(\mathbf{l})}{\partial \ell_2}\Big|_{\ell_1 = 1} = 0 \;\wedge\; \frac{\partial J(\mathbf{l})}{\partial \ell_3}\Big|_{\ell_1 = 1} = 0 \right\}, \tag{12}$$

$$\mathscr{L}_2 = \left\{ \mathbf{l} : \frac{\partial J(\mathbf{l})}{\partial \ell_1}\Big|_{\ell_2 = 1} = 0 \;\wedge\; \frac{\partial J(\mathbf{l})}{\partial \ell_3}\Big|_{\ell_2 = 1} = 0 \right\}, \tag{13}$$

Each set contains the solutions for a system of two polynomials of degree three, which has at most nine solutions. Since complex-valued solutions are not acceptable, the union of real solutions in these sets are denoted by $\bar{\mathscr{L}}$. The global optimum is given by

$$\mathbf{l}_i = \underset{\mathbf{l} \in \bar{\mathscr{L}}}{\arg\min}\, J_i(\mathbf{l}), \quad i = 1, \ldots, k. \tag{14}$$

There are at most 18 points in $\bar{\mathscr{L}}$ to be evaluated. These estimates of common tangents can be used as new cluster heads for iterative refinement.

5. DISCUSSION

5.1. Complexity Analysis

The number of tangent lines found and added to Hough accumulator is proportional to the number of SBR paths. The size of Hough space does not depend on the number of nodes or paths. Therefore, image processing steps in initial clustering method after quantization do not depend on the problem size. In the iterative refinement phase, the number of iterations do not depend on the problem size. In both assignment and fitting steps, the number of calculations for each of m clusters is proportional to the number of SBR paths. Hence, the overall complexity of the algorithm is m times the number of SBR paths, which becomes $O(m^2n^2)$.

5.2. High-order Reflections

Separating SBR paths from higher-order specular paths is not studied in this paper. Higher-order reflections are typically more attenuated, and can be mostly eliminated by thresholding. A number of methods are available in the literature which find SBR paths by testing different combinations of detected specular paths [15]. Another approach would be to start with an over-estimated model and eliminate higher-order reflections in the iterative refinement stage.

6. RESULTS

Simulation results for different stages of the algorithm are presented in this section. In the following simulation, distance estimation error is normally-distributed with zero mean and standard deviation of 0.1. Tangents to the ellipses shown in figure 3 are sampled, with 1000 tangents to each ellipse, and added to a Hough accumulator. The accumulator grid is 500×500 with $\rho \in [0, 10]$ and $\theta \in [-\pi, \pi]$. Figure 4a shows the Hough image after Gaussian filtering. The parameters of Gaussian filter, diameter = 15 and $\sigma = 4$, are chosen experimentally to get best results. For better visualization of Hough space, the ellipses are translated such that the origin is in the center of map. Figure 4b shows Hough image after thresholding and dilation. All clusters are detected in this image. Threshold value is found by a simple heuristic approach. The values of bins in Hough accumulator are sorted. Then, the k-th largest value with some large k is selected as a threshold level, $k = 200$ in this simulation. A flat disk-shaped *structural elements*, with radius = 10, is used for dilation. This size is chosen experimentally to get best results. Figure 5 shows the initial estimates of the reflector lines, along with the final estimates after refinement. The initial estimates are the centroids peak regions in Hough space. The iterative stages of assignment and fitting, improves the estimates. Solving a system of cubic equations is not trivial. A numerical solver is used in this experiment to solve the equations (12) and (13). The refinement stage converge very fast in two or three iterations. The performance of the algorithm depends on the network geometry and distance estimation error. The algorithm estimates unbounded lines instead of line segments, which is sufficient for multipath-aided localization. Moreover, line segments may be estimated by finding the intersections of lines.

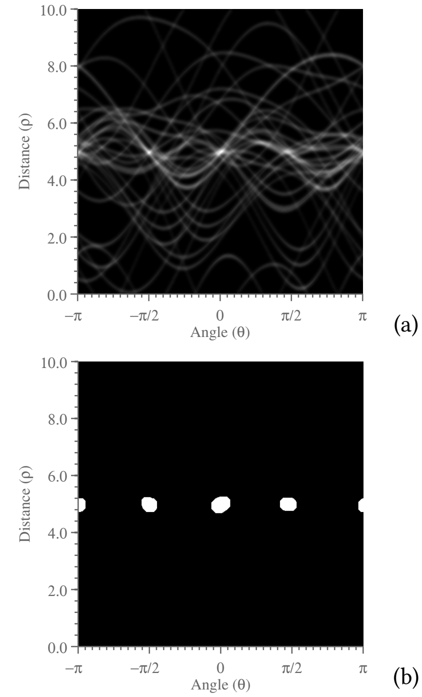

Fig. 4: (a) Hough accumulator space with sampled tangent lines after Gaussian filtering. Intensity peaks indicate common tangents. Note that θ is periodic, and $-\pi$ and π are overlapping points. (b) Binary mask of intensity peaks obtained after thresholding the Hough accumulator and dilation. Detected peak regions at $-\pi$ and π belong to the same cluster.

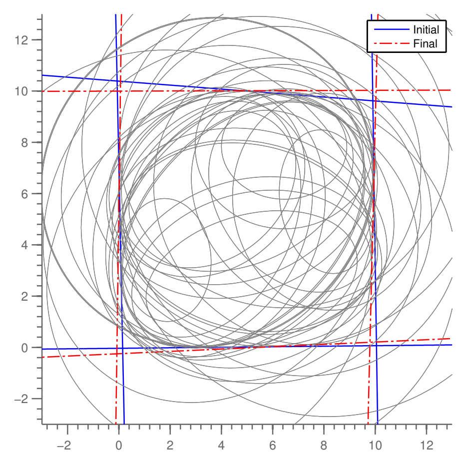

Fig. 5: Initial and final estimates of tangent lines. Iterative refinement improves the estimates, and final results closely match the true map.

7. CONCLUSIONS

Building a map of environment using multipath delay measurements is a challenging task. In this paper we formulated this problem as a clustering task, and proposed a novel low-complexity algorithm to solve it. The method starts with initial clustering based on a modified Hough transform. Then, an iterative refinement stage converges to the final estimate of the map. The proposed algorithm can be used for indoor mapping in wireless networks. Future studies will address the problem of simultaneous localization and mapping in wireless networks.

8. REFERENCES

[1] Hassan Naseri, Màrio Costa, and Visa Koivunen, "Multipath-aided cooperative network localization using convex optimization," *48th Annual Asilomar Conference on Signals, Systems, and Computers, 2014*, 2014.

[2] M. Froehle, Erik Leitinger, P. Meissner, and K. Witrisal, "Cooperative multipath-assisted indoor navigation and tracking (Co-MINT) using UWB signals," *IEEE ICC 2013 Workshop on Advances in Network Localization and Navigation (ANLN)*, 2013.

[3] Li Li and Jeffery L Krolik, "Simultaneous target and multipath positioning," *IEEE Journal of Selected Topics in Signal Processing*, vol. 8, no. 1, pp. 153–165, Feb 2014.

[4] R Zetik, H Yan, E Malz, S Jovanoska, G Shen, RS Thomä, R Salman, T Schultze, R Tobera, I Willms, et al., "Cooperative localization and object recognition," *UKoLoS – Ultra-Wideband Radio Technologies for Communications, Localization and Sensor Applications*, pp. 978–953, 2013.

[5] Andreas F Molisch, *Wireless communications*, John Wiley & Sons, 2010.

[6] Hassan Naseri, Màrio Costa, and Visa Koivunen, "A generalized formulation for harmonic retrieval in correlated noise," *48th Annual Conference in Information Sciences and Systems (CISS 2014)*, Mar 2014.

[7] Hassan Naseri, Jussi Salmi, and Visa Koivunen, "Synchronization and ranging by scheduled broadcasting," *IEEE Int'l Conference on Acoustics, Speech and Signal Processing (ICASSP 2013)*, 2013.

[8] Tobias Deissler and Jörn Thielecke, "UWB SLAM with Rao-Blackwellized Monte Carlo data association," in *Int'l Conference on Indoor Positioning and Indoor Navigation (IPIN 2010)*. IEEE, 2010, pp. 1–5.

[9] Vincenzo La Tosa, Benoît Denis, and Bernard Uguen, "Joint anchor-less tracking and room dimensions estimation through IR-UWB peer-to-peer communications," in *IEEE Int'l Conference on Ultra-Wideband (ICUWB 2011)*. IEEE, 2011, pp. 575–579.

[10] M Des Noes and B Denis, "Benefits from cooperation in simultaneous anchor-less tracking and room mapping based on impulse radio-ultra wideband devices," in *19th Int'l Conf. on Systems, Signals and Image Processing (IWSSIP 2012)*. IEEE, 2012, pp. 17–21.

[11] Wenyu Guo, Nick P Filer, and Rudolf Zetik, "Indoor mapping and positioning using impulse radios," in *Proc. IEEE/ION Position Location and Navigation Symposium (PLANS)*, 2006, pp. 153–163.

[12] Viktoria Pammer and Klaus Witrisal, "Ultra wideband communication system as sensor technology for 3D mapping," in *IEEE 17th Int'l Symposium on Personal, Indoor and Mobile Radio Communications*. IEEE, 2006, pp. 1–5.

[13] Heinrich Luecken and Armin Wittneben, "UWB radar imaging based multipath delay prediction for NLOS position estimation," in *IEEE Int'l Conference on Ultra-Wideband (ICUWB 2011)*. IEEE, 2011, pp. 101–105.

[14] Fabio Antonacci, Jason Filos, Mark RP Thomas, Emanuël Anco Peter Habets, Augusto Sarti, Patrick A Naylor, and Stefano Tubaro, "Inference of room geometry from acoustic impulse responses," *IEEE Transactions on Audio, Speech, and Language Processing*, vol. 20, no. 10, pp. 2683–2695, 2012.

[15] Ivan Dokmanić, Reza Parhizkar, Andreas Walther, Yue M Lu, and Martin Vetterli, "Acoustic echoes reveal room shape," *Proceedings of the National Academy of Sciences*, vol. 110, no. 30, pp. 12186–12191, 2013.

[16] Richard O Duda and Peter E Hart, "Use of the Hough transformation to detect lines and curves in pictures," *Communications of the ACM*, vol. 15, no. 1, pp. 11–15, 1972.